

Article

# Evaluation of Deep Learning Models for Image-Based Classification of Timber Logs by Market Value

Matevž Triplat \* , Žiga Lukančič and Vasja Kavčič

Slovenian Forestry Institute, Večna pot 2, 1000 Ljubljana, Slovenia; ziga.lukancic@gozdis.si (Ž.L.); vasja.kavcic@gozdis.si (V.K.)

\* Correspondence: matevz.triplat@gozdis.si; Tel.: +386-1-200-78-06

## Abstract

The identification of standing tree species, timber logs, and on-site assessment of their quality and value using images holds significant potential for forestry applications, including inventory management, traceability under EU regulations like the Deforestation Regulation, and market valuation amid growing demands for sustainable practices. This study addresses this by classifying images of timber logs by tree species and market value using the Orange data mining software, which leverages pre-trained convolutional neural networks (Inception v3 and SqueezeNet) to generate embeddings from a dataset of 5549 images collected at a real timber auction in Slovenia, followed by logistic regression image classification. Results show high accuracy for tree species classification (up to 92.6%), but substantially lower accuracy for market value classification (40%–55%), reflecting the greater complexity of value determination from visual features. These findings underscore the promise of deep learning for species identification while indicating the need for further methodological advancements to enhance value classification reliability, which offers the practical impact for operational forestry and bioeconomy value chains.

**Keywords:** image classification; timber quality; high value assortments; auctions; wood products; convolutional neural networks (CNNs); non-destructive evaluation; machine learning in forestry; tree species image recognition; forest wood assortment value

## 1. Introduction

Image analysis is used in many fields every day, from unlocking our smartphones with facial recognition to medical diagnostics. Yet, while its integration into the forestry sector remains relatively nascent, the potential for applying image analysis in forestry is considerable, including for low-cost tree volume estimation from single images [1], digitising operational processes with individual tree data [2], and accurate stem diameter and straightness measurement [3]. Traditional methods for wood identification and assessment often rely on laborious manual inspection, which is prone to inconsistency and error, particularly with large volumes. The emergence of deep learning techniques offers a promising avenue for automated, scalable, and more accurate classification of wood assortments and defects [4,5]. Deep learning models, such as convolutional neural networks and modern transformer-based architectures, have already been effectively applied to classify very high-resolution forest images, estimate tree height from multi-spectral satellite imagery, and differentiate forest types over time [6–8]. Moreover, image analysis, particularly using deep learning models such as convolutional neural networks, opens up new possibilities



Academic Editors: Kazuhiro Aruga and Rodolfo Picchio

Received: 27 February 2026

Revised: 16 April 2026

Accepted: 17 April 2026

Published: 23 April 2026

**Copyright:** © 2026 by the authors. Licensee MDPI, Basel, Switzerland. This article is an open access article distributed under the terms and conditions of the [Creative Commons Attribution \(CC BY\) license](https://creativecommons.org/licenses/by/4.0/).

for wood traceability, enabling log identification from end-face images under varying post-harvest conditions, lighting, and angles [8,9].

The EU's policy landscape further underscores the importance of such technologies. For instance, the EU Forest Strategy for 2030 emphasises innovation through strategic research, monitoring, and digitalisation to enhance forest resilience, multifunctional use, and bioeconomy value chains [10]. Meanwhile, the EU Deforestation Regulation mandates strict traceability and documentation to ensure commodities such as wood are deforestation-free and legally sourced [11]. This regulatory context creates a compelling incentive for deploying image analysis, machine learning, and deep learning tools in forestry [12]. Specifically, automated detection of harvesting activities [13], monitoring canopy changes, and identifying tree species [14] could serve as timely, scalable, and non-destructive methods to support EUDR due diligence, risk assessments, and sustainable forest management strategies [12], while enhancing traceability to combat illegal logging [15]. In particular, deep learning models, leveraging their capacity to learn intricate feature representations from raw data, address the limitations of traditional methods in scalability and robustness for complex forestry tasks [16]. This includes applications such as predictive analytics for forecasting forest dynamics, carbon sequestration, and species distribution, as well as enabling consistent tree monitoring systems for assessing carbon stocks and attributing changes to underlying drivers [17]. Such advanced capabilities position deep learning as a transformative technology for achieving sustainable forest management [17].

For instance, Jain et al. [18] successfully employed various transfer learning architectures for skin cancer detection, achieving strong results that underscore the adaptability of deep learning methods across domains. Building on such cross-domain successes, recent advances in deep learning have demonstrated remarkable capabilities in the visual classification of biological structures, with clear potential for forestry applications.

Several studies have successfully applied computer vision and deep learning to wood and tree identification. For example, Grondin et al. [19] used supervised end-to-end deep learning for tree detection and diameter estimation in forests, attaining 90.4% tree detection precision, 87.2% segmentation precision, and centimeter-level accuracy in keypoint estimations. Similarly, deep learning has identified tree species from angiosperm xylem images, surpassing the accuracy limitations of traditional wood anatomical methods [20], and classified tree species using multispectral airborne laser scanning data, outperforming conventional machine learning techniques [21].

Deep learning has also advanced traceability and assortment classification. For instance, deep learning methods have been applied to sawn timber surface quality evaluation [14]. Likewise, deep learning techniques have been applied to analyse CT images of logs [4]. Holmström et al. [22] demonstrated log identification from end-face images taken at varying post-harvest times, lighting conditions, and angles, while Vihlman et al. [9] evaluated deep learning models for identifying spruce and pine logs from images, providing insights into real-world performance. Lu et al. [23] measured log diameters and volumes using a deep learning-based model on truck and yard images, reporting a 1.2% volume error, and Wimmer et al. [8] applied a two-stage CNN to digital log end images for wood log recognition, reinforcing deep learning's role in timber tracing. Qualitative evaluation of logs for sale is particularly important, as it determines market value and optimal allocation based on qualitative characteristics, enabling premium pricing for high-quality timber logs, fair seller compensation, and buyer confidence in auctions [24,25]. Manual visual inspections, the traditional method, are labour-intensive, subjective, and expertise-dependent [25], underscoring the need for research into automated image-based systems, whose potential advantages include objective, remote, rapid, and scalable classification [25], enhancing pricing accuracy, operational efficiency, and bioeconomy value chains. These findings suggest

that deep learning has the capacity to support robust timber tracking systems. This broad application of deep learning in forestry, encompassing everything from defect detection to species identification and volume estimation, highlights its potential for revolutionizing timber logs classification by market value.

While previous studies have mainly applied deep learning techniques to tree species identification, the application of deep learning for classifying timber logs by market value using image analysis requires further investigation [14]. Therefore, this study addresses this gap by investigating whether the Orange data analysis tool can effectively identify tree species and evaluate timber log value from field images. Beyond species recognition, classifying timber logs by value is more complex because it depends on several parameters, including tree species, assortment dimensions, shape, and defects such as cracks and knots. Accordingly, this study specifically assesses the feasibility of identifying tree species and evaluating value through computer-based analysis of timber logs' field images. The objective of this study is not to model the full economic value formation process, but to assess whether visually observable features alone contain sufficient signal to support partial discrimination of value categories. In real-world applications, timber log value depends on multiple additional factors that are not captured in image data. Ultimately, this research aims to advance the practical applications of image recognition tools in forestry, particularly for value-based classification.

## 2. Materials and Methods

### 2.1. Sample Description

In this study, we used the timber log images, which were taken in 2023 at the 17th auction of the most valuable timber logs in Slovenj Gradec, Slovenia [26]. Auctions are used to sell high-quality assortments and can achieve high prices for valuable timber products. The total value of successful offers was approximately 2.9 million EUR, with an average (median) price of 359 EUR/m<sup>3</sup>. The most expensive assortment sold was sycamore, valued at 23,487.20 EUR (14,960.00 EUR/m<sup>3</sup>). The auction organizers supplied a database encompassing key assortment attributes, including diameter, length, volume, tree species, number of offers, and the winning bid. Timber log data were obtained from this auction database [27]. A catalogue of the auction results is publicly available in the form of a published book, while the underlying structured dataset (e.g., XLSX format) is maintained by the organizers and can be made available upon reasonable request to the auction organizers. The value of each log was defined as the final auction sale price per cubic meter (EUR/m<sup>3</sup>), obtained from the official auction database.

Images were captured with different cameras (Nikon D7000 (Nikon Corporation, Tokyo, Japan), iPhone 11 Pro (Apple Inc., Cupertino, CA, USA), and Canon PowerShot G3 X (Canon Inc., Tokyo, Japan)), producing resolutions of 4928 × 3264, 3024 × 4032, and 3648 × 5472 pixels, respectively. These were captured before the auction results were known. Image capture was completed over two days in February 2023, resulting in an initial dataset of 6043 timber log images. Each timber log at the auction was marked with an identification plate, visible in the photographs. In Adobe Lightroom Classic (version 12.2), the images were processed only in terms of file organization and cropping. File names were renamed to match the identification codes on the plates. No additional image enhancements (e.g., brightness, contrast, or color adjustments) were applied. Images were visually inspected during preprocessing, but no systematic filtering or exclusion based on image quality was performed. Although identification plates were visible in the images, they contained only numeric identifiers that were not systematically associated with the target classes (species or value), and thus could not be used by the model for meaningful classification. Images were also cropped horizontally to cover only the individual timber

log, minimizing the background. The images were manually processed by a single operator by cropping them along the width. Manual cropping was applied as a controlled preprocessing step to isolate the timber log from the background and reduce irrelevant variability. This procedure serves as a proxy for segmentation and ensures that the model focuses on the object of interest. While performed manually in this study, such preprocessing could be replaced by automated segmentation methods in operational applications. The images were cropped up to the edges of the log, so that each photograph contains the entire log. The formal criterion is that the centrally positioned log is fully captured in the image, with the edge of the log always included, while the remaining width of the image is removed as much as possible. The space left between the edge of the log and the edge of the image may slightly vary.

File sorting was performed in Python (version 3.11.1). The first four digits of each file name were parsed and converted to integers. Using the pandas module (version 1.5.3), information from the auction database was merged with the timber log images by ID, adding tree species information. The database was then filtered to exclude tree species represented by fewer than 100 images, resulting in a final dataset of 5549 images used in the analysis. Using the Python os and shutil modules, files were copied into folders corresponding to tree species.

Table 1 presents the timber log collection, which contains sub-collections of images of nine different tree species. Because Pedunculate oak and Sessile oak images are morphologically very similar (distinguishable only by leaves or fruits) [28], they were also grouped into a single sub-collection labelled “Oak”. Thus, we defined two collections: A1, comprising eight sub-collections (with Pedunculate and Sessile oak combined), and A2, comprising nine sub-collections (with Pedunculate and Sessile oak treated separately). As the auction did not represent all tree species equally, the number of images per species varied (from 125 images of Pear to 2634 images of Sessile oak). Despite this class imbalance, we decided to use all remaining images to maximise the available data and avoid unnecessary data loss. When Pedunculate and Sessile oak were combined, the Oak sub-collection contained 2909 images. The descriptive statistics presented in Table 1 (e.g., diameter, length, volume, and total value) were directly derived from this auction database.

**Table 1.** Summary statistics of log timber logs by tree species based on the auction database (standard deviation in brackets).

Scientific Name	Common Name	Number of Images	Average Diameter (cm)	Average Length (cm)	Average Volume (m <sup>3</sup> )	Total Volume (m <sup>3</sup> )	Total Value (EUR)
<i>Fraxinus excelsior</i> L.	Common ash	381	49.84 (13.20)	547.06 (196.62)	1.11 (0.68)	424.80	86,882.28
<i>Juglans regia</i> L.	Common walnut	136	48.35 (12.61)	406.40 (151.99)	0.78 (0.44)	106.28	59,460.61
<i>Larix decidua</i> Mill.	European larch	161	45.20 (9.22)	720.93 (234.60)	1.18 (0.61)	190.44	65,545.07
<i>Picea abies</i> (L.) Karst.	Norway spruce	837	58.90 (9.60)	598.21 (209.87)	1.66 (0.79)	1385.87	447,271.80
<i>Pyrus pyraaster</i> (L.) Burgsd.	Pear	123	41.72 (10.69)	342.93 (104.39)	0.50 (0.30)	61.63	15,712.23
<i>Quercus robur</i> L.	Pedunculate oak	275	56.33 (12.67)	461.96 (125.53)	1.22 (0.67)	334.36	257,048.30
<i>Quercus petraea</i> (Matt.) Liebl.	Sessile oak	2634	46.20 (11.92)	540.69 (189.31)	0.94 (0.55)	2477.51	1,172,523.40
<i>Acer pseudoplatanus</i> L.	Sycamore	898	47.64 (9.01)	556.71 (184.15)	1.01 (0.48)	911.67	353,101.97
<i>Ulmus glabra</i> Huds.	Wych elm	104	48.78 (12.09)	557.40 (196.85)	1.12 (0.68)	116.33	57,097.28
Total		5549				6008.89	2,514,642.94

The timber logs of four tree species were classified by market value: Norway spruce, Sessile oak, European larch, and Sycamore. Only tree species with sufficient sample sizes were included in the value classification analysis to allow reliable subdivision into value-

based quartiles and ensure robust model performance. Within each tree species collection, images were divided into quartiles based on assortment value per m<sup>3</sup> (Table 2). Timber logs of each tree species were then sorted into folders by quartile: 1st quartile (lowest 25%), 2nd and 3rd quartiles combined (25%–75%), and 4th quartile (highest 25%).

**Table 2.** Average values of European larch, Norway spruce, Sessile oak, and Sycamore timber logs.

Scientific Name	Common Name	Number of Images (n)	Total Number of Winning Bids (n)	Mean (EUR/m <sup>3</sup> )	SD (+/-)	MIN (EUR/m <sup>3</sup> )	Q1 (EUR/m <sup>3</sup> )	Q2 (EUR/m <sup>3</sup> )	Q3 (EUR/m <sup>3</sup> )	MAX (EUR/m <sup>3</sup> )
<i>Larix decidua</i> Mill.	European larch	161	233	292.70	140.90	96	223.50	263.50	321	1155
<i>Picea abies</i> (L.) Karst.	Norway spruce	837	1246	280.00	166.40	78	202	244	261	1530
<i>Quercus petraea</i> (Matt.) Liebl.	Sessile oak	2634	3983	400.20	254.50	81	260	357	460.50	2050
<i>Acer pseudo-platanus</i> L.	Sycamore	898	1201	286.20	929.10	71	118	138	189	14,960

Figure 1 shows one example of each tree species from the timber log collection, photographed at the auction.



**Figure 1.** GLS images from the auction. From left to right: Pedunculate oak, Wych elm, Sycamore, Sessile oak, Pear, European larch, Common walnut, Norway spruce, Common ash.

## 2.2. Statistics and Method

For this study, we used the Orange software tool (version 3.38.1) [29]. Orange is a free, open-source visual programming environment that democratizes image analytics by integrating deep models with small-scale machine learning [30].

Figure 2 depicts the workflow for image classification. The Import Images widget imported images, and the Image Embedding widget converted them to vector representations, which generated a data table. Image Embedding uses activations from the penultimate layer of a pre-trained convolutional neural network to represent images as feature vectors for supervised machine learning workflows [30]. This approach leverages CNNs' robust feature extraction to transform complex visual data into a format suitable for classification and regression [31]. The Image Embedding widget offers various pre-trained embedders (e.g., SqueezeNet, Inception v3, VGG-16, VGG-19, Painters, DeepLoc) and allows processing locally or on a remote server. We used Inception v3 and SqueezeNet (an efficient ImageNet-trained model achieving AlexNet-level accuracy with 50 times fewer parameters) [30]. The convolutional neural networks were not trained on this dataset but used as fixed feature extractors, allowing effective application even with relatively limited data.

The pre-trained Inception v3 and SqueezeNet models were used as fixed feature extractors within the Orange framework. No modifications or fine-tuning of the network weights were performed.

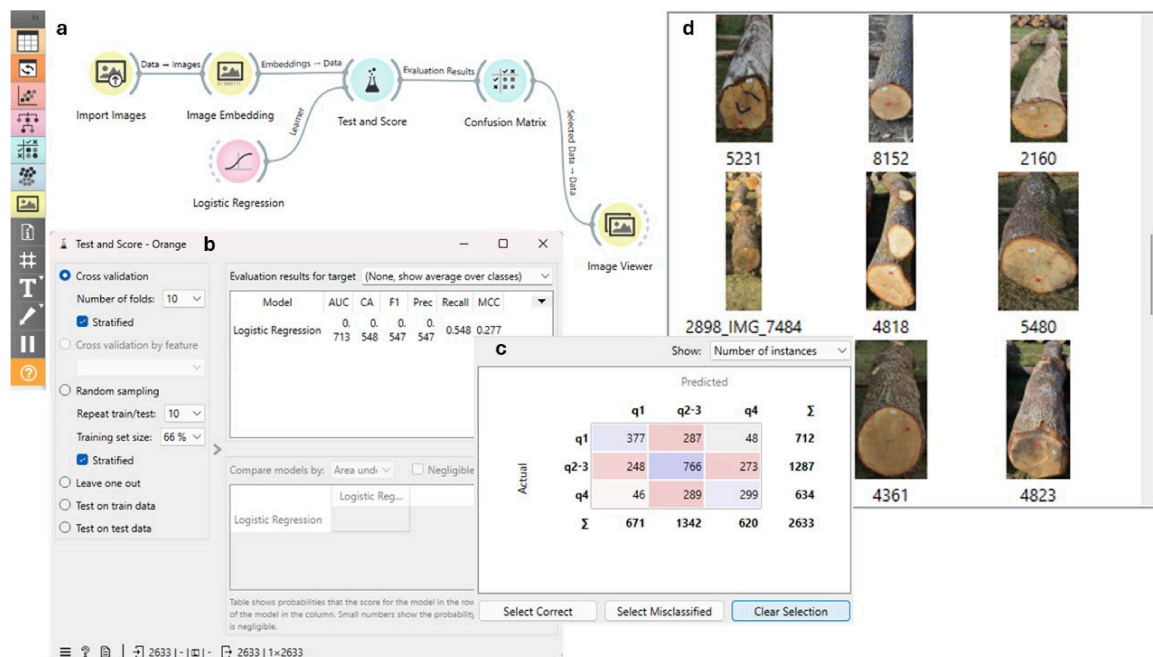


**Figure 2.** Workflow of the image classification process (image source: Orange screenshot). (a) The data analysis workflow begins with importing images from a local directory. The images are then processed using the Image Embedder, configured with different deep neural network models (Inception v3 and SqueezeNet). The resulting vector-based embeddings are passed to a cross-validation procedure, and (b) the evaluation results are forwarded to the Confusion Matrix widget (c). The confusion matrix provides information on classification performance and misclassification patterns. Selecting a specific cell in the confusion matrix triggers the transfer of the corresponding images and their descriptors to the Image Viewer (d) for further inspection. Color shading is used to improve readability of the confusion matrix. Blue tones indicate correct classifications along the diagonal (darker shades represent higher values), while red tones indicate misclassifications outside the diagonal (darker shades represent higher frequencies of errors).

The Test and Score widget then applied logistic regression on the embedded data, providing performance metrics such as classification accuracy, area under the ROC curve, F1-score, precision, recall, and Matthews correlation coefficient. These can be further analyzed via ROC curves or confusion matrices. AUC quantifies a model’s ability to discriminate between classes (0–1 scale;  $\geq 0.8$  indicates strong performance). Classification Accuracy (CA) measures the proportion of correctly classified instances, reflecting how closely a set of predictions aligns with their true values. F1-score (F1) is the harmonic mean of precision and recall [32]. Precision (Precision) refers to the ratio of true positives among all instances predicted as positive. Recall (Recall) indicates the proportion of true positive instances out of all actual positive instances in the dataset. The Matthews Correlation Coefficient (MCC) considers true and false positives and negatives and is widely recognized as a balanced metric suitable even when class distributions are highly uneven. These metrics are calculated based on Equations (1)–(5).

$$CA = \frac{TP + TN}{TP + TN + FP + FN} \tag{1}$$

$$F1 = \frac{2TP}{2TP + FP + FN} \tag{2}$$

$$\text{Precision} = \frac{TP}{TP + FP} \quad (3)$$

$$\text{Recall} = \frac{TP}{TP + FN} \quad (4)$$

$$\text{MCC} = \frac{TP \times TN - FP \times FN}{\sqrt{(TP + FP)(TP + FN)(TN + FP)(TN + FN)}} \quad (5)$$

where  $TP$  represents true positives,  $TN$  true negatives,  $FP$  false positives, and  $FN$  false negatives.

We repeated classifications 10 times across varied train-test partitions to assess reliability [33]. The Learner supports multiple sampling methods (e.g., cross-validation, random sampling, leave-one-out). Here, we applied stratified 10-fold cross-validation: the dataset was divided into 10 folds, ensuring that class proportions were preserved in each fold. Each fold was used once for testing, while the remaining folds were used for training. Logistic regression with L2 regularization ( $C = 1$ ) was used for testing.

The reported values (e.g., classification accuracy, AUC, F1-score) represent the mean performance across all folds. In the last step, the Confusion Matrix widget was used to visualize the performance of the classification models, illustrating the counts of true positive, true negative, false positive, and false negative predictions. The reported values are based on the aggregated predictions from the cross-validation procedure, providing an overall view of classification performance across all folds. Several combinations of image collections, embedders, and attributes were evaluated, as summarized in Table 3.

**Table 3.** Combinations of image collection, image embedder, and classification attribute (A1 = dataset with Pedunculate and Sessile oak combined; A2 = dataset with Pedunculate and Sessile oak treated separately).

Dataset	Image Embedder	Classification Attribute	Number of Images
A1	Inception v3	Tree species	5549
A2	Inception v3	Tree species	5549
A1	SqueezeNet	Tree species	5549
A2	SqueezeNet	Tree species	5549
European larch	Inception v3	Value	161
Norway spruce	Inception v3	Value	837
Sessile oak	Inception v3	Value	2634
Sycamore	Inception v3	Value	896

### 3. Results

#### 3.1. Different Combinations and Classification Models

The results of classifying the two datasets (A1, A2) by tree species, as well as individual timber log datasets (European larch, Norway spruce, Sessile oak, and Sycamore) by value, are summarized in Table 4. For the timber log collection (A1), where Pedunculate and Sessile oak were combined, classification accuracy by tree species was 92.6% using the Inception v3 embedder and 90.4% using SqueezeNet. When Pedunculate oak and Sessile oak were treated as separate species (A2), accuracy dropped to 79.1% (Inception v3) and 70.1% (SqueezeNet), representing decreases of 13.5 and 20.3 percentage points, respectively. In contrast, the lowest accuracy was obtained when assortments were classified by value, which was consistently lower than the accuracy of classifying samples A1 and A2 by tree species. European larch assortments were most accurately classified by value (55.3%), followed by Sessile oak (54.8%). Norway spruce (40.4%) was the least accurate.

**Table 4.** Statistical data of sample classification (A1 = dataset with Pedunculate and Sessile oak combined; A2 = dataset with Pedunculate and Sessile oak treated separately).

Dataset	Embedder	AUC	CA	F1	Prec	Recall	MCC
A1	Inception v3	0.993	0.926	0.925	0.924	0.926	0.889
A2	Inception v3	0.945	0.791	0.783	0.779	0.791	0.702
A1	SqueezeNet	0.991	0.904	0.904	0.903	0.904	0.857
A2	SqueezeNet	0.911	0.701	0.703	0.706	0.701	0.585
European larch	Inception v3	0.694	0.553	0.553	0.554	0.553	0.319
Norway spruce	Inception v3	0.568	0.404	0.401	0.400	0.404	0.076
Sessile oak	Inception v3	0.713	0.548	0.547	0.547	0.548	0.277
Sycamore	Inception v3	0.608	0.452	0.450	0.450	0.452	0.124

### 3.1.1. Classification of Timber Logs by Tree Species

For each image, Orange predicted the corresponding tree species. The classification results for dataset A1 using the Inception v3 embedder are presented numerically in Table 5. Wych elm was the least accurately classified. Out of 104 timber logs, only 53 were correctly identified. For comparison, Table 6 shows the results where Pedunculate oak and Sessile oak were treated as separate species. Pedunculate oak was correctly classified 66 times, but incorrectly classified as Sessile oak 192 times. In total, there were 275 Pedunculate oak images. Sessile oak performed much better: out of 2634 images, 2337 were correctly classified, and only 117 were misclassified as Pedunculate oak.

**Table 5.** Classification Results for Dataset A1. The table presents absolute values and relative values (in brackets).

		Predicted							
		Common Ash	Common Walnut	European Larch	Norway Spruce	Oak	Pear	Sycamore	Wych Elm
Actual	Common ash	305 (80.1%)	0 (0%)	2 (0.5%)	36 (9.4%)	12 (3.1%)	1 (0.3%)	9 (2.4%)	16 (4.2%)
	Common walnut	7 (5.1%)	103 (75.7%)	4 (2.9%)	0 (0%)	10 (7.4%)	10 (7.4%)	1 (0.7%)	1 (0.7%)
	European larch	1 (0.6%)	2 (1.2%)	130 (80.7%)	17 (10.6%)	5 (3.1%)	3 (1.9%)	2 (1.2%)	1 (0.6%)
	Norway spruce	17 (2.0%)	0 (0%)	4 (0.5%)	796 (95.1%)	8 (1.0%)	2 (0.2%)	4 (0.5%)	6 (0.7%)
	Oak	6 (0.2%)	3 (0.1%)	2 (0.1%)	12 (0.4%)	2835 (97.5%)	0 (0%)	50 (1.7%)	1 (0%)
	Pear	8 (6.5%)	9 (7.3%)	5 (4.1%)	4 (3.3%)	8 (6.5%)	87 (70.7%)	0 (0%)	2 (1.6%)
	Sycamore	2 (0.2%)	0 (0%)	1 (0.1%)	2 (0.2%)	58 (6.5%)	1 (0.1%)	831 (92.5%)	3 (0.3%)
	Wych elm	27 (26.0%)	0 (0%)	1 (1.0%)	11 (10.6%)	5 (4.8%)	4 (3.8%)	3 (2.9%)	53 (51.0%)

Color shading is used to improve readability of the confusion matrix. Blue tones indicate correct classifications along the diagonal (darker shades represent higher values), while red tones indicate misclassifications outside the diagonal (darker shades represent higher frequencies of errors).

**Table 6.** Classification Results for Dataset A2. The table presents absolute values and relative values (in brackets).

		Predicted								
		Common Ash	Common Walnut	European Larch	Norway Spruce	Pear	Pedunculate Oak	Sessile Oak	Sycamore	Wych Elm
Actual	Common ash	206 (54.1%)	2 (0.5%)	0 (0%)	21 (5.5%)	1 (0.3%)	6 (1.6%)	74 (19.4%)	56 (14.7%)	15 (3.9%)
	Common walnut	4 (2.9%)	95 (69.9%)	0 (0%)	0 (0%)	6 (4.4%)	2 (1.5%)	27 (19.9%)	1 (0.7%)	1 (0.7%)
	European larch	1 (0.6%)	0 (0%)	104 (64.6%)	8 (5%)	1 (0.6%)	3 (1.9%)	43 (26.7%)	1 (0.6%)	0 (0%)
	Norway spruce	12 (1.4%)	0 (0%)	5 (0.6%)	709 (84.7%)	3 (0.4%)	9 (1.1%)	63 (7.5%)	35 (4.2%)	1 (0.1%)
	Pear	2 (1.6%)	6 (4.9%)	2 (1.6%)	4 (3.3%)	68 (55.3%)	2 (1.6%)	31 (25.2%)	7 (5.7%)	1 (0.8%)
	Pedunculate oak	5 (1.8%)	2 (0.7%)	1 (0.4%)	7 (2.5%)	0 (0%)	66 (24%)	192 (69.8%)	0 (0%)	2 (0.7%)
	Sessile oak	40 (1.5%)	6 (0.2%)	10 (0.4%)	64 (2.4%)	11 (0.4%)	117 (4.4%)	2337 (88.7%)	36 (1.4%)	13 (0.5%)
	Sycamore	26 (2.9%)	0 (0%)	2 (0.2%)	34 (3.8%)	3 (0.3%)	1 (0.1%)	32 (3.6%)	783 (87.2%)	17 (1.9%)
	Wych elm	21 (20.2%)	2 (1.9%)	0 (0%)	4 (3.8%)	2 (1.9%)	1 (1%)	25 (24%)	28 (26.9%)	21 (20.2%)

Color shading is used to improve readability of the confusion matrix. Blue tones indicate correct classifications along the diagonal (darker shades represent higher values), while red tones indicate misclassifications outside the diagonal (darker shades represent higher frequencies of errors).

### 3.1.2. Classification of Timber Logs by Value

Table 7 shows the classification results of timber logs by value. The most accurate classification was obtained for European larch (55.3%), followed by Sessile oak, with 1442 out of 2634 timber logs correctly classified (54.8%). Norway spruce was the least accurate, with 338 of 837 timber logs correctly classified (40.4%). Overall, classification of timber logs by value was considerably less accurate than classification by tree species.

**Table 7.** Sorting of timber logs by value (collections of European larch, Norway spruce, Sessile oak, and Sycamore). Absolute and relative values (in brackets) are shown.

		Predicted					
		European Larch			Norway Spruce		
Actual		q1	q2-3	q4	q1	q2-3	q4
	q1	27 (58.7%)	13 (28.3%)	6 (13%)	75 (33.3%)	98 (43.6%)	52 (23.1%)
	q2-3	15 (22.4%)	35 (52.2%)	17 (25.4%)	78 (21.5%)	182 (50.1%)	103 (28.4%)
	q4	2 (4.2%)	19 (39.6%)	27 (56.3%)	52 (20.9%)	116 (46.6%)	81 (32.5%)
		Sessile oak			Sycamore		
		q1	q2-3	q4	q1	q2-3	q4
	q1	377 (52.9%)	287 (40.3%)	48 (6.7%)	83 (38.8%)	103 (48.1%)	28 (13.1%)
	q2-3	248 (19.3%)	766 (59.5%)	273 (21.2%)	87 (20.3%)	225 (52.4%)	117 (27.3%)
	q4	46 (7.3%)	289 (45.6%)	299 (47.2%)	21 (8.3%)	135 (53.4%)	97 (38.3%)

Color shading is used to improve readability of the confusion matrix. Blue tones indicate correct classifications along the diagonal (darker shades represent higher values), while red tones indicate misclassifications outside the diagonal (darker shades represent higher frequencies of errors).

## 4. Discussion

In this study, we investigated the feasibility of image-based machine learning to identify tree species and estimate the value of timber logs from digital images. The primary objective was to determine whether the Orange image analytics environment, employing pre-trained deep learning models such as Inception v3 for image embedding and logistic regression, could deliver accurate and practical results for forestry tasks like tree species identification and timber log value estimation. This approach proved effective, achieving 92.6% classification accuracy for the timber logs collection (A1 dataset) using Inception v3, outperforming SqueezeNet (90.4%). Our study reached a similar accuracy to a study on log ends under varying conditions such as ageing and lighting (91%) [22]. This methodology relied on Inception v3 embeddings, followed by logistic regression with L2 regularization and 10-fold cross-validation, facilitating robust assessment of model generalization, crucial for real-world forestry applications amid diverse log characteristics, lighting, aging, and orientations [22].

Specifically, our study extended beyond simple classification by evaluating timber log collection based on market value, a complex task that requires a nuanced understanding of wood properties and market dynamics. Moreover, the results underscore the efficacy of deep learning in classifying wood species, consistent with prior research demonstrating high accuracy in similar classification tasks using convolutional neural networks [34]. For instance, earlier work has shown that deep convolutional neural networks can achieve up to 98.2% accuracy in classifying 11 common hardwood species from longitudinal section images [34]. However, it should be noted that such results are obtained under controlled imaging conditions using prepared wood samples and are therefore not directly comparable to the present study, which is based on field-acquired images of timber logs under variable conditions. Our findings nevertheless support the applicability of deep learning approaches for wood species classification, particularly for species such as Pedunculate

oak and European larch, where the Inception v3 model exhibited strong predictive capabilities, including 92.6% accuracy on dataset A1 with combined oak species and up to 95% correct classifications for Norway spruce in confusion matrices. The observed differences in classification performance between datasets can be partly explained by class separability. When morphologically similar species (e.g., Pedunculate oak and Sessile oak) are treated as separate classes, the feature space becomes more complex, increasing overlap between classes and reducing overall classification accuracy, even for other species. This highlights a general limitation of image-based classification in forestry, where subtle visual differences between species can significantly affect model performance.

While many other image recognition platforms exist, we did not explore them in depth due to limitations such as proprietary restrictions, reduced model control, or lack of support for architectures like InceptionV3. Orange applies transfer learning by freezing all CNN layers and using the network as a fixed feature extractor, followed by training a separate classifier on the extracted features. For deeper domain adaptation, frameworks like Keras, TensorFlow, or PyTorch would allow unfreezing layers or building custom models from scratch, potentially improving accuracy. However, these approaches require significantly more computational resources, time, and data, which may not be feasible in early-stage or resource-constrained studies. In the study, we used and compared different embedders, similar to Vacek et al. [4], who conducted research on wood species classification. Classification accuracy was higher for three of the four main datasets when using the InceptionV3 embedder than SqueezeNet.

Furthermore, the findings revealed substantial differences in classification performance depending on the image source and classification target. For example, leaf-based classification achieved the highest accuracy, with both Inception v3 and SqueezeNet exceeding 98%. This performance is consistent. The use of herbarized leaves photographed on a uniform background likely contributed to this performance, as field images would introduce significantly more variability in lighting, background, and leaf condition. Nevertheless, the near-perfect results demonstrate that leaf morphology remains a powerful visual discriminator for tree species identification when high-quality images are available.

Similarly, studies utilizing transfer learning for plant disease classification [35] and plant species identification from leaf venation patterns have demonstrated robust performance, reinforcing the utility of such methods in botanical contexts [36].

Classification from timber log images proved challenging, particularly when distinguishing morphologically similar species such as Pedunculate Oak and Sessile Oak. Treating them separately dropped accuracy to 79.1% (13.5 percentage point decrease; Table 4), with frequent confusions such as 192 Pedunculate Oaks misclassified as Sessile oak. Meanwhile, species with distinctive external features, such as Norway spruce (~95% correct; Table 5) or Sycamore (~93% correct; Table 5), were consistently classified with high accuracy, highlighting that feature distinctiveness remains a decisive factor in classification success. This study intentionally isolates image-based information to evaluate its standalone contribution to value classification. By contrast, classification of assortments by value produced much lower accuracy, with no species exceeding 55.3% correct predictions (e.g., 55.3% European larch, 40.4% Norway spruce; Table 4). The lower performance observed in value-based classification reflects the fact that timber log value is influenced by multiple non-visual factors that are not captured in image data. In this study, the model intentionally relies only on visual information to assess its standalone predictive potential. The results therefore highlight the limitations of image-only approaches and underscore the need for integrating additional data sources in future research. This limitation reflects the complexity of value determination, which in real-world timber markets depends on multiple factors, including size, form, defects, and market-specific grading rules. In the context

of high-value timber auctions, the highest price categories often correspond to exceptional assortments, meaning that value-based classification can partially reflect underlying quality differences rather than only general market fluctuations. However, in this study, these factors were not explicitly included as input variables, as the classification was based solely on image data. As evidenced by frequent confusions across quartiles in Table 7, and the limited representativeness of the dataset from the Slovenj Gradec auction. The auction assortments were not representative of broader market conditions, potentially introducing bias into the training data. Furthermore, value-based grading relies on features that are not easily captured in images, such as internal wood quality or subtle surface defects. This aligns with Achatz et al. [31], who achieved only 80% accuracy for quality classes even when augmenting images with numerical data (e.g., length, diameter). As a result, purely image-based valuation is currently not robust enough for operational use without supplementary non-visual data. Classification assigns images to predefined classes. Even assuming bid prices reflect defects, market value is continuous and cannot form discrete classes. Thus, quartiles capture a spectrum of values rather than pure categories. Further research is therefore imperative to develop and test methods for timber log valuation based on continuous values, such as regression models calibrated against market prices, or refined classifications targeting precisely defined, objectively detectable defects (e.g., knots, sweep, soft rot, and decay).

Overall, the results suggest that image-based deep-learning classification, as implemented in Orange, can achieve operationally relevant accuracy for tree species identification under controlled conditions. A limitation of this study is that it is based on a single dataset derived from a specific timber auction and on embedding models available within the Orange framework. While the use of pre-trained embeddings enables effective analysis of relatively small datasets, the restriction to a subset of species and a single auction dataset limits the generalizability of the results. The findings should therefore be interpreted as a context-specific baseline rather than a universally applicable model. This was a deliberate design choice aimed at evaluating the applicability of accessible, off-the-shelf tools for forestry practice. Nevertheless, this choice also limits the generalizability of the results beyond similar auction-based datasets and constrains the ability to explore more advanced or customizable deep learning approaches. However, extending such methods to timber log value estimation remains a considerable challenge. To address this, future work should explore multimodal approaches that combine image analysis with other data sources, such as 3D scanning, provenance data, or manual defect grading, to improve value prediction performance [31]. Additionally, testing on more diverse and in-field image datasets will be necessary to validate model robustness under real operational constraints. Beyond the application of pre-trained models such as Inception v3 and SqueezeNet, which were originally trained on generic datasets such as ImageNet, a promising direction would be the development of a domain-specific deep-learning model trained directly on forestry data annotated with known assortment values. Such a model could learn fine-grained features of wood quality and assortment characteristics that are not present in general-purpose image datasets, potentially enabling more accurate value-based classification. While this approach would require compiling a large, representative dataset of assortments with precisely defined value labels, it would represent a significant step towards a practical and scalable solution for automated timber logs valuation in forestry.

The timber log images occasionally contained other samples in the background, which may have influenced the classification results. Additionally, some timber logs lacked bark or had bark damage, further affecting image quality. In our view, these factors likely reduced classification accuracy. The dataset used in this study is characterized by class imbalance, which may influence classification performance, particularly for underrepresented species.

Although stratified cross-validation was applied to preserve class distributions across folds, no additional balancing techniques were used to maintain the original data structure. Future work should explore strategies such as class weighting or data augmentation to further improve performance on minority classes.

## 5. Conclusions

While prior studies have predominantly utilized deep learning for tree species identification from leaves, bark, or canopy images and for tree health diagnostics [37,38], this study adopts a more expansive and original framework. In addition to species classification, it pioneers the categorization of wood timber logs by market value, a particularly formidable and essential challenge in operational forestry [39,40]. Market value appraisal extends beyond visual attributes to encompass dimensions, morphology, and internal wood properties, which are challenging to derive from images alone [41,42]. Consequently, the findings demonstrate exceptionally high accuracy for tree species classification but suboptimal performance for timber log valuation, reflecting the intricate, multidimensional nature of value assessment that hinges on partially non-visual characteristics indiscernible from imagery.

These outcomes carry critical implications. Image-based deep learning techniques are presently suitable for practical species recognition in quality assurance, biodiversity monitoring, and digital forest inventories [31]. Conversely, the limited efficacy in value classification highlights a pivotal research gap: developing reliable image-centric systems for economic valuation of timber logs requires substantial advances, particularly in integrating non-visual inputs and curating more representative, annotated datasets [31]. Future studies should prioritize multimodal fusion, such as 3D laser scanning for precise dimensional quantification and acoustic sensors for internal flaw detection, to enrich visual inputs and improve value prediction [31]. Moreover, expanding datasets to include greater species diversity (especially those with subtle similarities), along with variability in provenance, cultivation practices, and imaging conditions, will be essential for building generalizable, robust wood classification models.

The experiments further confirm that advanced architectures like Inception v3 achieve high accuracy [14,22,43], though lightweight networks can offer competitive performance with efficient resource use [44], particularly when inter-class similarities are pronounced. However, simpler models remain viable for tasks involving visually distinct species. Thus, careful selection of architectures, balancing complexity with computational efficiency, is crucial for effective deployment across diverse forestry applications.

From a practical perspective, the results underscore promising applications of image-based deep learning classification in forestry operations. The high accuracy in tree species identification [22,37,38] supports tasks such as timber sorting, quality control, and digital forest inventories, enabling rapid, non-destructive, and scalable assessments [31]. These methods could also enhance traceability and transparency in timber supply chains, aligning with regulations like the EU Deforestation Regulation by automating consistent documentation of origin and characteristics. Conversely, the suboptimal performance in assortment value classification highlights the limitations of image-only approaches for reliable economic log assessment [39,40], as value depends on non-visual factors like dimensions and internal defects [41,42]. Operational systems should thus integrate images with complementary data, such as dimensional measurements [23], defect detection [14,45], or expert grading, to enable multimodal value prediction. This hybrid strategy would bolster decision-making in timber markets and forest management, paving the way for automated grading systems that optimize resource use and sustainability [5].

Despite these insights, the study faced several limitations. While the use of pre-trained embeddings enables effective analysis of relatively small datasets, the restriction to a subset of species and a single auction dataset limits the generalizability of the results. The findings should therefore be interpreted as a context-specific baseline rather than a universally applicable model. In addition, the dataset is characterized by a modest sample size and class imbalance across timber log images. Additionally, the uniform capture conditions (with limited variation in illumination, perspectives, and backgrounds) may hinder model generalization to uncontrolled field environments. Future research should explore segmentation-based approaches to more precisely isolate individual logs from the background, which may further improve classification performance. Future research should rigorously test these approaches on larger, more diverse, and real-world datasets to assess operational viability. Developing a forestry-specific model trained on domain-relevant data annotated with timber log values also holds great promise. Unlike generic pre-trained networks from broad image repositories, such models could capture specialized wood quality and defect features, enabling precise, deployable value estimation. Although curating such datasets is resource-intensive, it promises substantial efficiency gains, enhanced timber market traceability, and greater transparency. Ongoing efforts will focus on improving accuracy and versatility through expanded log imagery covering more species, sizes, and conditions, thereby strengthening generalization [23]. Ultimately, advances in data acquisition and deep learning stand to transform traditional timber grading into efficient, automated systems [45], optimizing resource use and supporting sustainable forest management [5].

**Author Contributions:** Conceptualization, M.T.; methodology, V.K. and M.T.; validation, Ž.L. and M.T.; formal analysis, Ž.L., V.K., and M.T.; resources, M.T.; data curation, Ž.L.; writing—original draft preparation, Ž.L.; writing—review and editing, Ž.L., V.K., and M.T.; visualization, Ž.L.; supervision, M.T. All authors have read and agreed to the published version of the manuscript.

**Funding:** Data collection for this study was co-funded by the Ministry of Agriculture, Forestry and Food of the Republic of Slovenia and the Slovenian Research and Innovation Agency, within the project “Efficient management of private forests to support wood mobilization” grant number V4-2013. The study was also supported by the research core group “Forest biology, ecology and technology” grant number P4-0107, financed by the Slovenian Research and Innovation Agency, and by the Development Fund of the Slovenian Forestry Institute.

**Data Availability Statement:** The data presented in this study are openly available in Digital repository of Slovenian research organisations and Zenodo at Triplat et al. [26].

**Acknowledgments:** The authors gratefully acknowledge the research assistants from the Department for Forest Technique and Economics at the Slovenian Forestry Institute for their support during fieldwork, as well as Tiama d.o.o., the organisers of the Slovenj Gradec auction, for providing detailed information on the sold assortments.

**Conflicts of Interest:** The funders had no role in the design of the study; in the collection, analyses, or interpretation of data; in the writing of the manuscript; or in the decision to publish the results.

## Abbreviations

The following abbreviations are used in this manuscript:

AUC	Area under the ROC (receiver-operating curve).
CA	Classification accuracy.
Prec	Abbreviation for precision, the proportion of true positives among all instances classified as positive.
Recall	The proportion of true positives among all positive instances in the data.
F1	A weighted harmonic mean of precision and recall.

MCC Matthew's correlation coefficient, which considers true and false positives and negatives and is generally regarded as a balanced measure even when the classes are of very different sizes.

## References

1. Yu, Z.; Zhang, B.; Ma, T.; Zhang, M.; Wang, S.; He, M.; Ji, W.; Li, H.; Feng, Z.; Wang, Z. Single-image estimation of tree volume via pixel-mapped 3D reconstruction: A low-cost solution using deep learning and curvature segmentation. *Sci. Total Environ.* **2025**, *1002*, 180420. [[CrossRef](#)] [[PubMed](#)]
2. Keefe, R.F.; Zimbelman, E.G.; Picchi, G. Use of Individual Tree and Product Level Data to Improve Operational Forestry. *Curr. For. Rep.* **2022**, *8*, 148–165. [[CrossRef](#)]
3. Tran, H.; Woeste, K.; Li, B.; Verma, A.; Shao, G. Measuring tree stem diameters and straightness with depth-image computer vision. *J. For. Res.* **2023**, *34*, 1395–1405. [[CrossRef](#)]
4. Vacek, O.; Gergel, T.; Bucha, T.; Gracovský, R.; Gejdoš, M. Automatic Wood Species Classification and Pith Detection in Log CT Images. *Forests* **2024**, *15*, 2207. [[CrossRef](#)]
5. Fard, F.H.; Fard, S.H.; Jonoobi, M. A Low-Cost Machine Learning Approach for Timber Diameter Estimation. *arXiv* **2025**. [[CrossRef](#)]
6. Bermudez, J.; Rogers, C.; Sothe, C.; Cyr, D.; Gonsamo, A. A Deep Learning Approach to Estimate Canopy Height and Uncertainty by Integrating Seasonal Optical, SAR and Limited GEDI LiDAR Data over Northern Forests. *arXiv* **2024**. [[CrossRef](#)]
7. Viennois, G.; Tulet, H.; Tresson, P.; Ploton, P.; Couteron, P.; Barbier, N. Sentinel-2 forest typology mapping in Central Africa: Assessing deep learning and image preprocessing effects. *Front. Remote Sens.* **2025**, *6*, 1682132. [[CrossRef](#)]
8. Wimmer, G.; Schraml, R.; Hofbauer, H.; Uhl, A. *Two-Stage CNN-Based Wood Log Recognition*; University of Applied Sciences Salzburg: Salzburg, Austria, 2021; 4p.
9. Vihlman, M.; Kulovesi, J.; Visala, A. Tree Log Identity Matching using Convolutional Correlation Networks. In *Proceedings of the 2019 Digital Image Computing: Techniques and Applications (DICTA), Perth, Australia, 2–4 December 2019*; IEEE: Piscataway, NJ, USA, 2020; pp. 1–8.
10. European Commission. *New EU Forest Strategy for 2030; Communication from the Commission to the European Parliament, the Council, the European Economic and Social Committee and the Committee of the Regions, COM(2021) 572 Final*; European Commission: Brussels, Belgium, 2021.
11. European Union. *Regulation (EU) 2023/1115 of the European Parliament and of the Council of 31 May 2023 on the Making Available on the Union Market and the Export from the Union of Certain Commodities and Products Associated with Deforestation and Forest Degradation and Repealing Regulation (EU) No 995/2010*; European Union: Brussels, Belgium, 2024.
12. Ali, G.; Mijwil, M.M.; Adamopoulos, I.; Ayad, J. Leveraging the Internet of Things, Remote Sensing, and Artificial Intelligence for Sustainable Forest Management. *Babylon. J. Internet Things* **2025**, *2025*, 1–65. [[CrossRef](#)]
13. Brandt, M.; Chave, J.; Li, S.; Fensholt, R.; Ciaia, P.; Wigneron, J.-P.; Gieseke, F.; Saatchi, S.; Tucker, C.J.; Igel, C. High-resolution sensors and deep learning models for tree resource monitoring. *Nat. Rev. Electr. Eng.* **2024**, *2*, 13–26. [[CrossRef](#)]
14. Wang, Y.; Zhang, W.; Gao, R.; Jin, Z.; Wang, X. Recent advances in the application of deep learning methods to forestry. *Wood Sci. Technol.* **2021**, *55*, 1171–1202. [[CrossRef](#)]
15. Longuetaud, F.; Pot, G.; Mothe, F.; Barthelemy, A.; Decelle, R.; Delconte, F.; Ge, X.; Guillaume, G.; Mancini, T.; Ravoajanahary, T.; et al. The TreeTrace Douglas database: Quality assessment and traceability of Douglas fir. In *Proceedings of the 3rd ECCOMAS Thematic Conference on Computational Methods in Wood Mechanics (CompWood 2023), Dresden, Germany, 5–8 September 2023*.
16. Wielgosz, M.; Berg, S.; Korpunen, H.; Hoffmann, S. Spatiotemporal Analysis of Forest Machine Operations Using 3D Video Classification. *arXiv* **2025**, arXiv:2505.24375. [[CrossRef](#)]
17. Wang, T.; Zuo, Y.; Manda, T.; Hwarari, D.; Yang, L. Harnessing Artificial Intelligence, Machine Learning and Deep Learning for Sustainable Forestry Management and Conservation: Transformative Potential and Future Perspectives. *Plants* **2025**, *14*, 998. [[CrossRef](#)] [[PubMed](#)]
18. Jain, S.; Singhanian, U.; Tripathy, B.; Nasr, E.A.; Aboudaif, M.K.; Kamrani, A.K. Deep Learning-Based Transfer Learning for Classification of Skin Cancer. *Sensors* **2021**, *21*, 8142. [[CrossRef](#)] [[PubMed](#)]
19. Grondin, V.; Fortin, J.-M.; Pomerleau, F.; Giguère, P.; Fassnacht, F. Tree detection and diameter estimation based on deep learning. *For. Int. J. For. Res.* **2023**, *96*, 264–276. [[CrossRef](#)]
20. Nieradzick, L.; Sieburg-Rockel, J.; Helmling, S.; Keuper, J.; Weibel, T.; Olbrich, A.; Stephani, H. Automating Wood Species Detection and Classification in Microscopic Images of Fibrous Materials with Deep Learning. *Microsc. Microanal.* **2024**, *30*, 508–520. [[CrossRef](#)]
21. Taher, J.; Hyyppä, E.; Hyyppä, M.; Salolahti, K.; Yu, X.; Matikainen, L.; Kukko, A.; Lehtomäki, M.; Kaartinen, H.; Thurachen, S.; et al. Multispectral airborne laser scanning for tree species classification: A benchmark of machine learning and deep learning algorithms. *arXiv* **2025**, arXiv:2504.14337. [[CrossRef](#)]

22. Holmström, E.; Raatevaara, A.; Pohjankukka, J.; Korpunen, H.; Uusitalo, J. Tree log identification using convolutional neural networks. *Smart Agric. Technol.* **2023**, *4*, 100201. [[CrossRef](#)]
23. Lu, Z.; Yao, H.; Lyu, Y.; He, S.; Ning, H.; Yu, Y.; Zhai, L.; Zhou, L. A Deep Learning Method for Log Diameter Measurement Using Wood Images Based on Yolov3 and DeepLabv3+. *Forests* **2024**, *15*, 755. [[CrossRef](#)]
24. Šebek, V.; Kupčák, V.; Janáková Sujová, A. Change in forest species composition and its projections into the economy of forest owners. *J. For. Sci.* **2024**, *70*, 368–380. [[CrossRef](#)]
25. Nocetti, M.; Aminti, G.; Vicario, M.; Brunetti, M. Assessment of Oak Roundwood Quality Using Photogrammetry and Acoustic Surveys. *Forests* **2025**, *16*, 421. [[CrossRef](#)]
26. Triplat, M.; Kavčič, V.; Jež, M. *Forest Log Assortments Photo Dataset from the 2023 Slovenj Gradec Timber Auction*; Slovenian Forestry Institute: Ljubljana, Slovenia, 2025. [[CrossRef](#)]
27. *Licitacija Vrednejših Sortimentov Lesa: Katalog Sortimentov = Wertholzsubmission: Vesteigerungskatalog*; Društvo Lastnikov Gozdov Mislinjske Doline: Slovenj Gradec, Slovenia; Zveza Lastnikov Gozdov Slovenije: Ljubljana, Slovenia, 2023.
28. Jurkšienė, G.; Baranov, O.Y.; Kagan, D.I.; Kovalevič-Razumova, O.A.; Baliuckas, V. Genetic diversity and differentiation of pedunculate (*Quercus robur*) and sessile (*Q. petraea*) oaks. *J. For. Res.* **2019**, *31*, 2445–2452. [[CrossRef](#)]
29. Demšar, J.; Curk, T.; Erjavec, A.; Gorup, Č.; Hočevar, T.; Možina, M.; Polajnar, M.; Toplak, M.; Starič, A.; Štajdohar, M.; et al. Orange: Data Mining Toolbox in Python. *J. Mach. Learn. Res.* **2013**, *14*, 2349–2353.
30. Godec, P.; Pancur, M.; Ilenic, N.; Copar, A.; Strazar, M.; Erjavec, A.; Pretnar, A.; Demšar, J.; Starič, A.; Toplak, M.; et al. Democratized image analytics by visual programming through integration of deep models and small-scale machine learning. *Nat. Commun.* **2019**, *10*, 4551. [[CrossRef](#)] [[PubMed](#)]
31. Achatz, J.; Lukovic, M.; Hilt, S.; Ladrach, T.; Schubert, M. Convolutional neural networks for quality and species sorting of roundwood with image and numerical data. *Expert Syst. Appl.* **2024**, *246*, 123117. [[CrossRef](#)]
32. Shin, S.J.; Kim, H.; Han, S.-T. Comparison of the Performance Evaluations in Classification. *IJARCCCE* **2016**, *5*, 441–444. [[CrossRef](#)]
33. Kobayashi, K.; Kegasa, T.; Hwang, S.W.; Sugiyama, J. Anatomical features of Fagaceae wood statistically extracted by computer vision approaches: Some relationships with evolution. *PLoS ONE* **2019**, *14*, e0220762. [[CrossRef](#)]
34. Wu, F.; Gazo, R.; Haviarova, E.; Benes, B. Wood identification based on longitudinal section images by using deep learning. *Wood Sci. Technol.* **2021**, *55*, 553–563. [[CrossRef](#)]
35. Sai, N.R.; Rao, T.S.; Kumari, G.L.A. Comparative Study on Reliability of Transfer Learning to Classify Plant-Based Diseases. *Int. J. Eng. Adv. Technol.* **2021**, *10*, 154–160. [[CrossRef](#)]
36. Bharadwaj, B.; Mishra, A.; Bharadwaj, S. Transfer Learning-Based CNN Models for Plant Species Identification Using Leaf Venation Patterns. *arXiv* **2025**, arXiv:2509.03729. [[CrossRef](#)]
37. Ecke, S.; Stehr, F.; Frey, J.; Tiede, D.; Dempewolf, J.; Klemmt, H.-J.; Endres, E.; Seifert, T. Towards operational UAV-based forest health monitoring: Species identification and crown condition assessment by means of deep learning. *Comput. Electron. Agric.* **2024**, *219*, 108785. [[CrossRef](#)]
38. Abreu-Dias, R.; Santos-Gago, J.M.; Martín-Rodríguez, F.; Álvarez-Sabucedo, L.M. Advances in the Automated Identification of Individual Tree Species: A Systematic Review of Drone- and AI-Based Methods in Forest Environments. *Technologies* **2025**, *13*, 187. [[CrossRef](#)]
39. Chen, S.; Yang, T.; He, X.; Cao, X.; Zhu, P.; Qiu, J. The evaluation of wood and its products based on the classi. *arXiv* **2023**. [[CrossRef](#)]
40. Gejdoš, M.; Gergel', T. Case study of qualitative sorting of raw wood assortments in the conditions of a forestry enterprise in Slovakia. *Cent. Eur. For. J.* **2022**, *68*, 232–237. [[CrossRef](#)]
41. Lukovic, M.; Ciernik, L.; Muller, G.; Kluser, D.; Pham, T.; Burgert, I.; Schubert, M. Probing the complexity of wood with computer vision: From pixels to properties. *J. R. Soc. Interface* **2024**, *21*, 20230492. [[CrossRef](#)]
42. Khazem, S.; Fix, J.; Pradalier, C. Improving Knot Prediction in Wood Logs with Longitudinal Feature Propagation. In Proceedings of the 14th International Conference on Computer Vision Systems—ICVS 2023, Vienne, Austria, 27–29 September 2023.
43. Singh, S.; Tyagi, B. Computational Comparison of CNN Based Methods for Violence Detection. 2023, *preprint*. [[CrossRef](#)]
44. Wadekar, S.N.; Chaurasia, A. MobileViTv3: Mobile-Friendly Vision Transformer with Simple and Effective Fusion of Local, Global and Input Features. *arXiv* **2022**, arXiv:2209.15159. [[CrossRef](#)]
45. Chun, T.H.; Hashim, U.R.a.; Ahmad, S. Timber Defect Identification: Enhanced Classification with Residual Networks. *Int. J. Adv. Comput. Sci. Appl.* **2024**, *15*, 0150468. [[CrossRef](#)]

**Disclaimer/Publisher's Note:** The statements, opinions and data contained in all publications are solely those of the individual author(s) and contributor(s) and not of MDPI and/or the editor(s). MDPI and/or the editor(s) disclaim responsibility for any injury to people or property resulting from any ideas, methods, instructions or products referred to in the content.